Reduction of Natural Frequency due to Flexural Cracks or Shear Cracks in Reinforced Concrete Members

S. Nagata, Y. Miyagawa & K. Kanazawa
Central Research Institute of Electric Power industry, Japan

SUMMARY:
This paper presents reduction of fundamental frequency in reinforcement concrete members due to flexural cracks or shear cracks. Four specimens, in which amount of the stirrups varied to obtain different failure modes, were constructed. Cyclic static loads were applied stepwisely to the specimens to induce seismic damage. Free vibration data of the damaged members was obtained by hammer impact test. Vibration characteristics at each damage state were successfully identified to clarify the relationships between damage levels and reductions of fundamental frequencies under various failure modes. The fundamental frequency was significantly decreased due to flexural cracks that accompanied with yield of longitudinal bars. This result indicates that yielding of reinforcements can be detected from reduction of natural frequency.

Keywords: Damage detection, Reinforced concrete, Natural frequency, Flexural crack, Shear crack

1. INTRODUCTION

When civil infrastructures suffer extensive damage due to an event of the strong earthquake, damage should be immediately detected and then its location and level adequately evaluated to make restoration go smoothly (Rytter 1993). Seismic damages are generally detected based on direct visible inspection, but damages are not always appeared clearly on surface of the structural members. And also even if some local damages are visibly detected, it is not always easy to assess adequately structural safety on a whole structural system. Vibration-based damage detection is considered to be one of effective measures that can overcome such a weakness of the visual inspection (Housner et al. 1997; Rens et al. 1997; Aktan et al. 2000). It is well known that vibration characteristics changes depending on the damage levels (Seki et al. 1996; Neild et al. 2002 and 2003). Therefore it is expected that this method will be effective especially for reinforced concrete structures.

Recently the measuring tools as well as the system identification techniques are significantly improved. Thus we can choose the several methods such as forced vibration test, free vibration test and ambient vibration test (Kanazawa et al. 2005 and 2008), depending on aim of measurements or surrounding conditions of structures. Nonetheless the practical use of these vibration tests is still limited. One of the reasons is probably that the number of research on damage and vibration property relation (Seki et al. 2003; Uehan and Meguro 2004; Nagata et al. 2009) is not enough to establish the damage criteria for various structures. Under present status it is not easy to assess structural damage smoothly from transition of modal properties, even though vibration data can be easily obtained and accumulated.

The work presented here investigates change of vibration properties such as natural mode shape and natural frequency of the reinforced concrete members, whose damages are induced by a series of cyclic loadings. Four reinforced concrete specimens were constructed for this experiment. Amounts of the stirrups are varied in these specimens to change dominant failure modes. Lateral cyclic loads were stepwisely increased to the specimens under constant vertical load. The fundamental natural frequency of the damaged members was obtained by hammer impact tests, in order to clarify the relationship between damage level and change of vibration characteristics due to flexural cracks or shear cracks.

2. EXPERIMENTAL CONDITIONS

2.1. Test Specimens

Table 1 presents properties of test specimens. Configurations of the specimen No.1 without stirrups and No.3 with stirrups are shown in **Fig.1**. Totally four specimens were constructed. Originally they were designed to represent center walls in box culvert (Miyagawa and Matumura 2011). The main difference of the specimen is the amounts of stirrups, while the other parameters such as the aspect ratios, the strength of the concrete and the reinforcements, the axial loads representing the dead loads were kept constant as far as possible. The stirrup ratios in No.1, No.2, No.3 and No.4 are 0%, 0.16%, 0.32% and 0.71% respectively. This increment of stirrups improves the shear capacity of the reinforced concrete members (Niwa et al. 1986). As a result, the ratio of flexural strength to shear strength are estimated at 0.67%, 0.99%, 1.32% and 2.06% respectively, so that their dominant failure modes change from shear failure to flexural failure.

Outward appearances are exactly same in all the specimens. Each of them consists of a beam element with rectangular cross section of 400mm by 800mm as a main member, and it was constructed between the top and bottom stabs. The heights of the beam without the haunches, with the haunches, and from center to center of the stubs, denoted by h_1, h_2, and h_3 in **Fig. 1**, are 1,200mm, 1,600mm and 2,050mm respectively. The same batch of concrete was casted in all the specimens, and their compressive strength at each test day was within a range of 34.5MPa to 36.3MPa. The longitudinal-bar ratio is 0.57%. The axial stress ratio, defined as a ratio of applied axial load to axial load capacity at a concrete section, ranged from 4.35% to 4.13%.

Table 1. Structural and material properties of test specimens.

	No. 1	No. 2	No.3	No.4
Compressive strength of concrete	34.5MPa	34.9MPa	36.3MPa	35.6MPa
Young's modulus of concrete	30.5GPa	30.2GPa	29.7GPa	29.1GPa
Longitudinal-bar ratio	0.57%	0.57%	0.57%	0.57%
Diameter of longitudinal bars	16mm	16mm	16mm	16mm
Yield stress of longitudinal bars	369MPa	369MPa	369MPa	369MPa
Stirrup ratio	0%	0.16%	0.32%	0.71%
Diameter of stirrups	-	6mm	6mm	10mm
Pitch of stirrups	-	200mm	100mm	100mm
Yield stress of stirrups	-	390.4MPa	390.4MPa	370.9MPa
Axial stress ratio	4.35%	4.30%	4.13%	4.21%
Shear strength of specimens	310.7kN	462.4kN	617.0kN	958.1kN
Flexural strength of specimens	465.7kN	465.8kN	466.1kN	465.9kN
Strength ratio of specimens	0.67%	0.99%	1.32%	2.06%

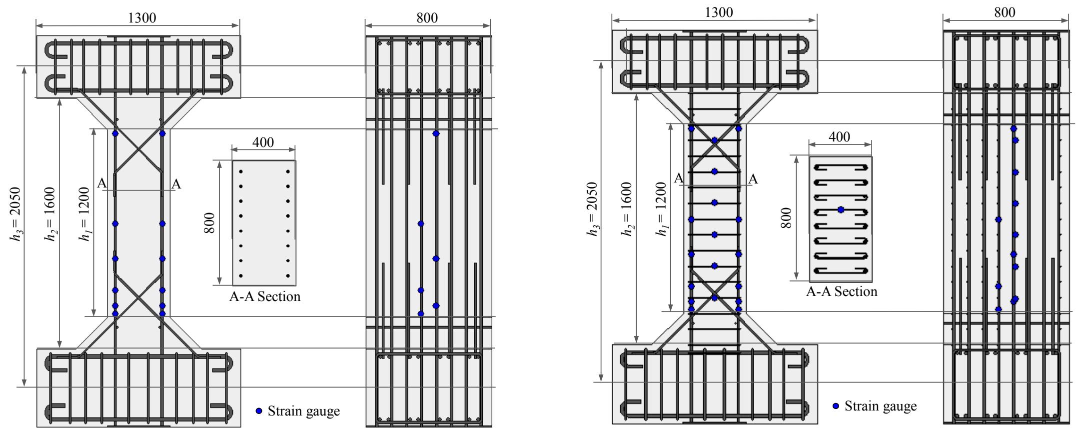

(a) Specimen without stirrups (No. 1)

(b) Specimen with stirrups (No. 3)

Figure 1. Configuration of test specimens (unit: mm).

2.2. Cyclic Loading Test

Fig.2 shows experimental setup to induce the seismic damage in the beam element of the specimens. The cyclic static loading was applied horizontally to the each specimen by a lateral actuator under displacement control. During the lateral cyclic loadings, constant vertical load corresponding to approximately 450kN was provided by two vertical actuators, and the rotation of the top stub was kept constant to induce an antisymmetric bending moment to the beam. Displacement was stepwisely increased until the specimen failed in shear or flexure. Lateral and vertical forces were measured by the load cells equipped in the lateral actuator and the vertical actuators respectively. Differential transformers were set on the top and bottom stubs to measure the relative displacements in horizontal and vertical directions. Strain gauges were attached to the longitudinal bars as well as stirrups as shown in **Fig.1** to monitor the yielding of these reinforcements.

2.3. Impact Vibration Test

Impact vibration tests were performed, as described in **Fig.3**, before loading and during unloading intervals of the cyclic loading paths. The impact excitation was applied at midspan of the beam element by using a plastic hammer. Totally 18 accelerometers were attached on the beam and the stubs in order to measure free vibration in the horizontal direction and to capture the fundamental natural mode shape as well as the natural frequency transition due to the seismic damage. In the vibration test the measuring range of the acceleration, the sampling frequency and the resolutions of the A/D conventions were 10,000 cm/s^2, 10 kHz, and 16 bit respectively.

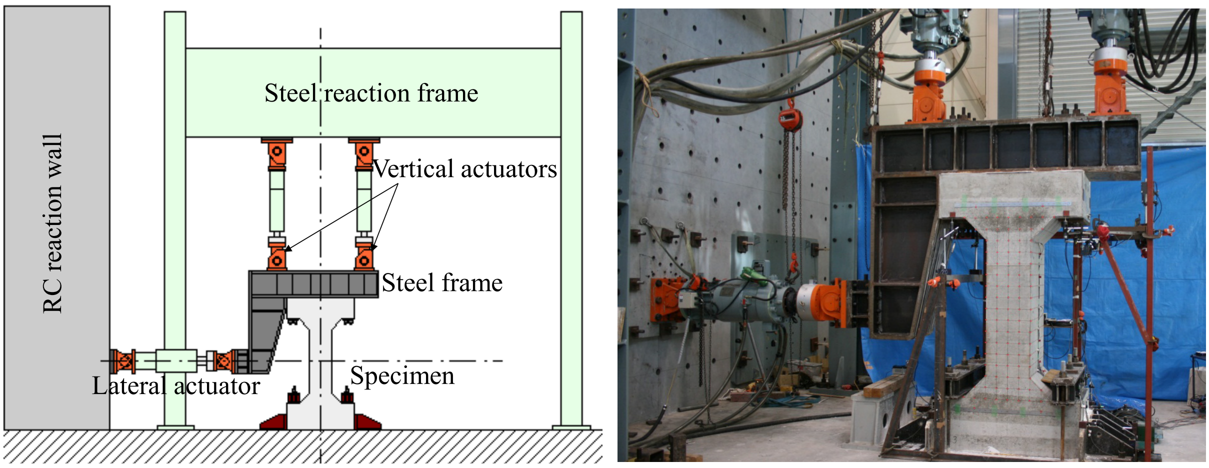

Figure 2. Experimental setup for cyclic loading test.

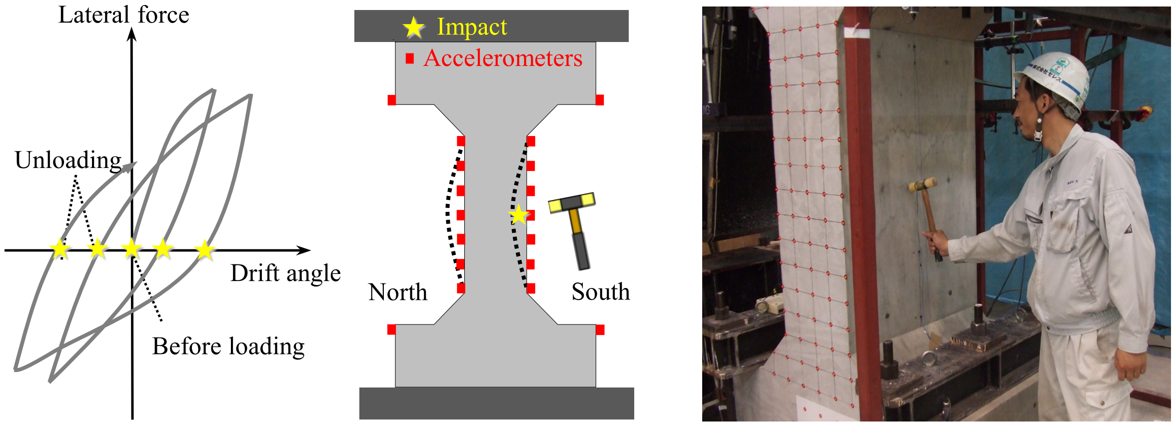

Figure 3. Hammer impact tests conducted at unloading intervals of cyclic loadings.

3. HYSTERETIC BEHAVIOR UNDER CYCLIC LOADINGS

Before discussing results of the impact vibration test, nonlinear hysteretic behaviour obtained from the cyclic loading test are presented to understand the basic features of damage states. **Fig. 4** shows the lateral force vs. drift angle hysteresis in all the specimens. The drift angle shown here is defined as ratio of the horizontal displacement to height from center to center of both stubs. In all the specimens, the longitudinal bars started to yield at 0.4% drift and then the restoring force reached almost maximum strength at 0.6% drift. After that, in No.1 without stirrup, the lateral strength significantly deteriorated at 0.9% drift, due to occurrence of shear cracks. In No. 2 and No.3, although shear cracks developed at -1.2% drift and -2.3% drift respectively, deterioration of strength was less significant in No.3 because of amount of stirrups. On the other hand shear cracks did not occur until 3% drift in No.4 with the highest stirrup ratio. It is obvious that, while the maximum strength was almost the same in all the specimens, the more stirrups were provided, the higher its ductility capacity became.

Relation between tangent stiffness and drift angle are plotted in **Fig.5**, which obtained from the hysteretic loops in **Fig.4**. Because general trend on deterioration of the stiffness was similar, the results in the specimen No.1 and No.4 were shown here. Based on the relations, although there seemed no obvious correlation between the deterioration of stiffness and events such as yield of reinforcements and occurrence of shear cracks, the stiffness decreased rapidly at lower drift angle within 1% but change of the stiffness is relatively small at higher drift angle.

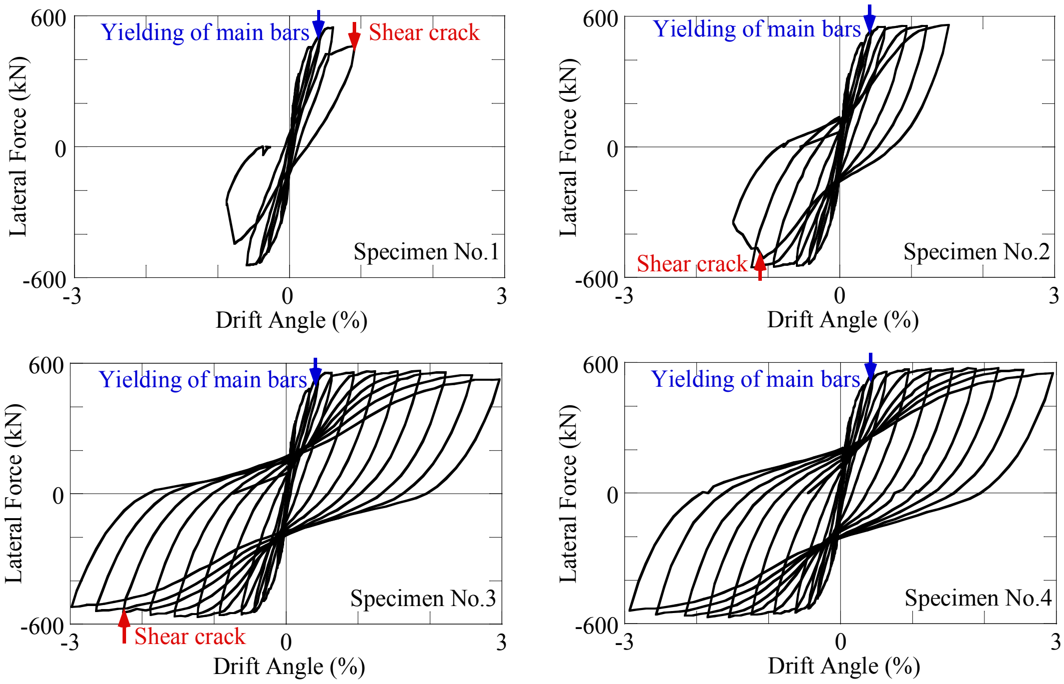

Figure 4. Lateral force and drift angle relations.

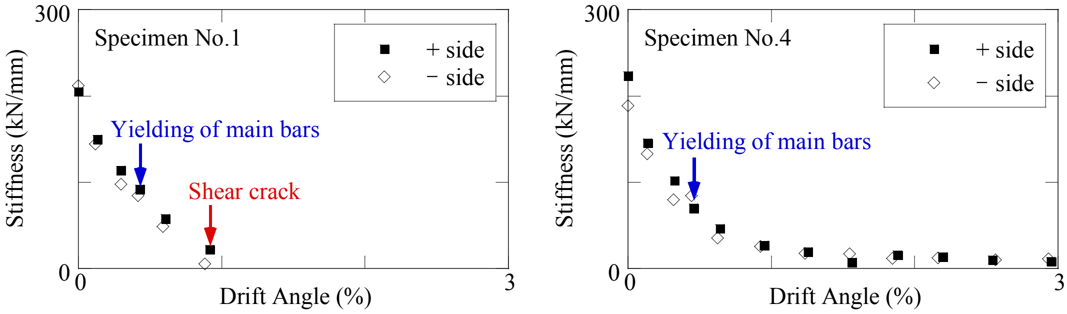

Figure 5. Relations between tangent stiffness and experienced maximum drift angle.

4. CHANGE OF VIBRATION PROPERTIES DUE TO SEISMIC DAMAGE

Relationships between seismic damage and change in vibration characteristic such as natural mode shapes and natural frequencies are discussed in this section. Especially to see effect of the different failures modes, test results obtained in the specimen No.1 without stirrups and No.4 with the highest stirrup ratio are mainly presented in the following.

4.1. Natural Mode Shapes

4.1.1. Specimen No.1 that failed in shear

Fig. 6 and **Fig.7** show the free vibration data, which were measured at middle height of the specimen No.1 without stirrups, in time domain and frequency domain respectively. To see change of vibration characteristic before and after shear cracks, the results at experienced maximum drift -0.6% and 0.9% drift are presented here. Progress of the damage at the corresponding experienced maximum drifts is presented in **Fig. 8**. At the experienced maximum drift of -0.6%, a clear free vibration with a single peak of 354Hz was obtained. The vibrations in the both north and south sides seem to have the same property. It is confirmed that the free vibration with the same dominant frequency could be obtained when the same impact vibration tests were performed at the same damage state in three times.

On the other hand, at 0.9% drift the dominant frequency decreased to 329Hz and the power spectral density (hereinafter called "PSD"), which represented intensity of vibration in the particular frequency, is obviously higher in the south side than that in the north side. In addition, second peak were appeared only at the south side of the specimen. **Fig. 9** presents natural mode shapes obtained by picking up the PSD of the dominant frequency from the vibration data measured at the 18 points shown in **Fig.3**. Before occurrence of shear cracks, the beam fixed at both ends with top and bottom stubs, seem to behave as one continuous body without any significant local vibration mode. However, the mode shape became more complex after occurrence of shear cracks. This is probably because local vibration modes developed around the potion damaged with the shear cracks.

4.1.2. Specimen No.4 that failed in flexure

Fig. 10 shows progress of flexural cracks observed in the specimen No.4 with the highest stirrup ratio at -0.1%, -0.6%, -1.9% and -2.9% drift. At -0.1% drift flexural cracks slightly developed around both end of the beam, but the reinforcing bars did not yield yet. The bars started to yield at 0.4% drift as previously described, and the flexural cracks became stepwise significant until -1.9% drift. Then exfoliation of concrete initiated at -1.9% drift. Finally, damage of concrete became extensive especially in the upper haunch at -2.9% drift as shown in **Fig.10** (d).

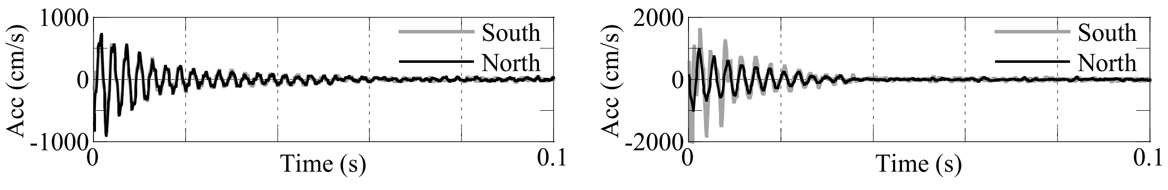

(a) Experienced maximum drift -0.6% (b) Experienced maximum drift 0.9%

Figure 6. Free vibration time history at middle height of specimen No.1 before and after shear cracks

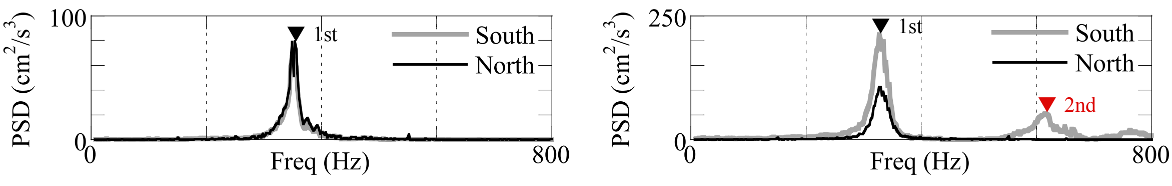

(a) Experienced maximum drift -0.6% (b) Experienced maximum drift 0.9%

Figure 7. Power spectrum on vibration data at middle height of specimen No.1 before and after shear cracks

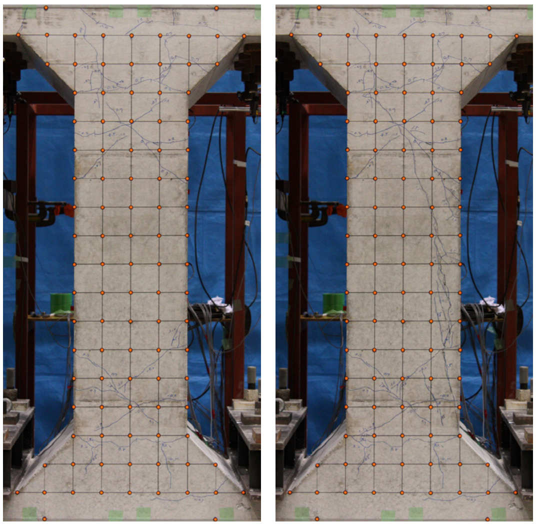

(a) -0.6% drift (b) 0.9% drift

Figure 8. Shear cracks developed in specimen No.1

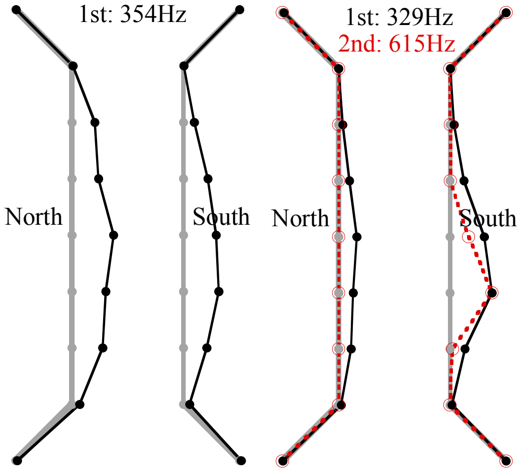

(a) -0.6% drift (b) 0.9% drift

Figure 9. Natural mode shapes in specimen No.1

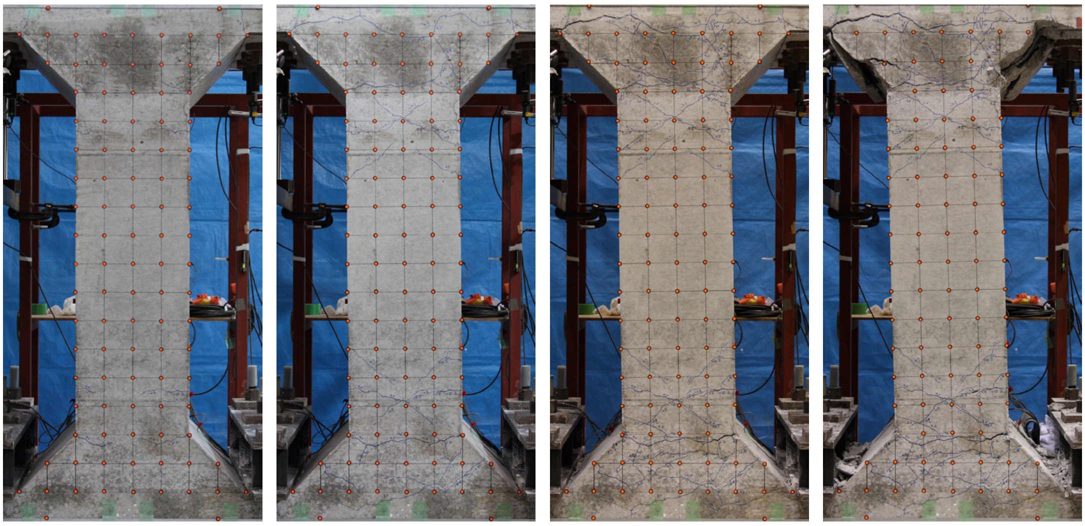

(a) -0.1% drift (b) -0.6% drift (c) -1.9% drift (d) -2.9% drift

Figure 10. Flexural cracks developed in specimen No.4

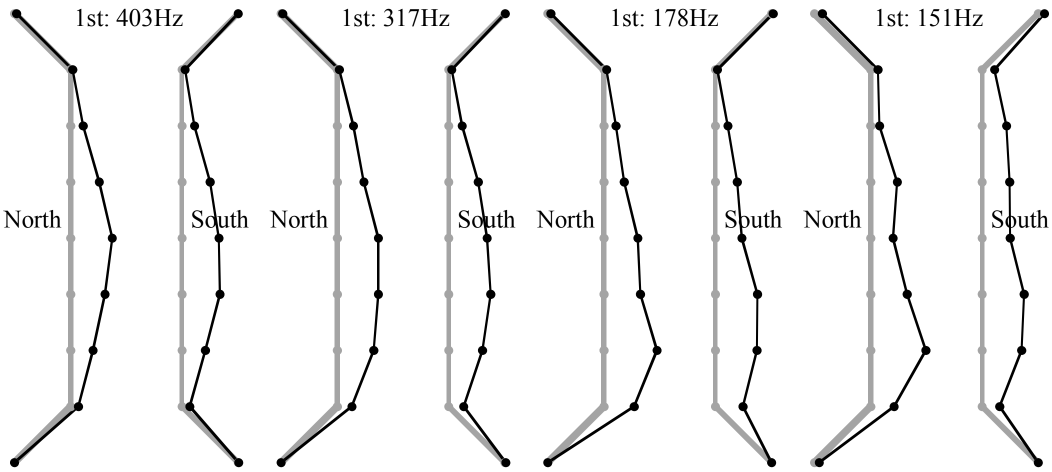

(a) -0.1% drift (b) -0.6% drift (c) -1.9% drift (d) -2.9% drift

Figure 11. Natural mode shapes of specimen No.4

The natural mode shapes at the corresponding damage states of -0.1%, -0.6%, -1.9% and -2.9% drift are shown in **Fig.11**. Firstly, the mode shapes at -0.1% drift, in which slight cracks initiated around both end of the beam element, was symmetric both horizontally and vertically. Then deformation around the bottom end of the beam became stepwisely significant until flexural failure. This indicated that local stiffness in the lower portion of structural member deteriorated more extensively than that in the upper portion during the cyclic loadings. However the mechanism of such a transition of the local stiffness cannot be explained well based on data presented herein. Therefore further investigation is required about more detailed distribution of deformation developed in the reinforced concrete member during the cyclic loadings.

4.2. Natural Frequencies

Reduction of the natural frequency of the specimens due to flexural cracks or shear cracks is presented here. The first natural frequency at each damage state, including the positive side and the negative side along with the loading direction, was estimated by peak picking in the power spectra. As a consequence the relationships between fundamental frequency and experienced maximum drift angle were successfully obtained for all the specimens as shown in **Fig.12**.

Firstly, the natural frequency at undamaged state (see points in 0% drift angle in **Fig.12**) was approximately 420Hz in all the specimens and the reduction was quite limited until yielding of the main reinforcements. The frequencies were significantly decreased just after the yielding of reinforcements at 0.4% drift. And also, in the range of 0.4% to 1.5% drift, the frequencies likely became lower at the negative side than those at the positive side in the same amplitude, probably because of effect of the cyclic loads. As mentioned in the previous section, shear cracks were developed in the specimen No.1, No.2 and No.3 at 0.9%, -1.5%, and -2.3% respectively, and this resulted in the deterioration of lateral strength drastically in No.1 and No.2. However the fundamental frequency seems to be less affected by such shear cracks based on the relations in **Fig.12**. In addition, although the exfoliation of concrete at the both end of beam initiated at about 2.0% drift and this became stepwisely extensive in the specimen No.3 and No.4, there existed almost no further reductions were recognized after 2.0% drift.

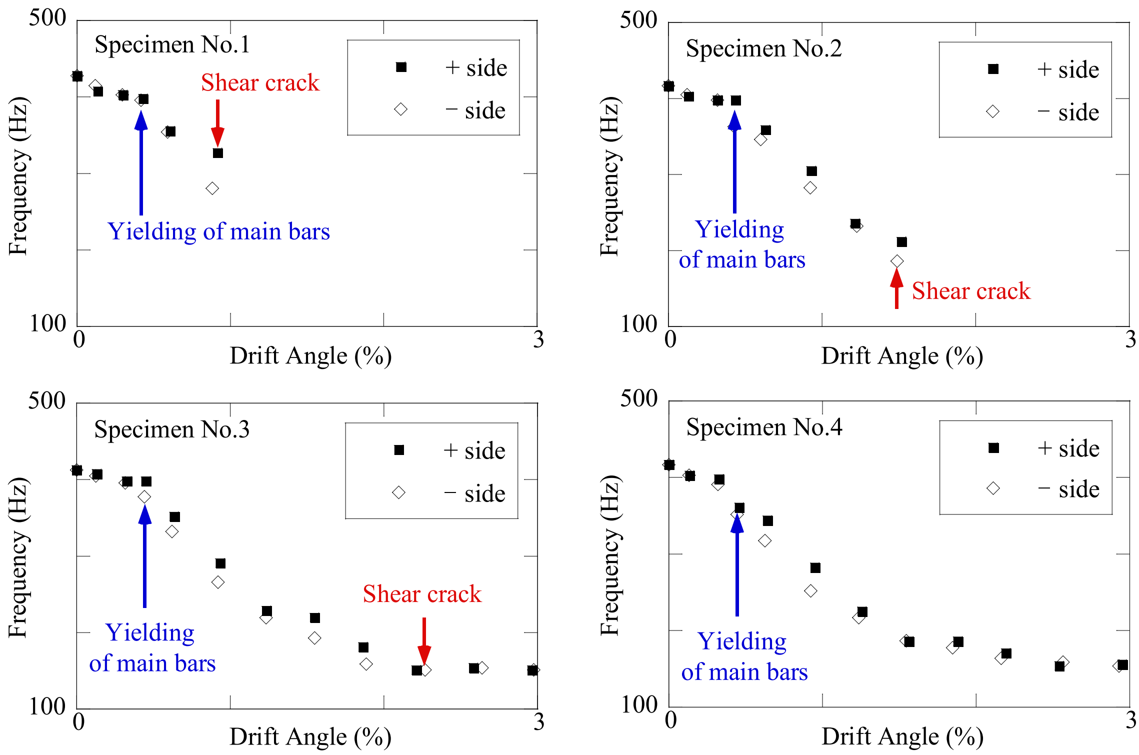

Figure 12. Relations between fundamental frequency and experienced maximum drift angle.

5. CONCLUTIONS

To clarify change of vibration characteristics due to flexural cracks or shear cracks, impact vibration tests were performed on the reinforced concrete specimens damaged by cyclic loading tests. Four specimens, in which amount of the stirrups varied respectively to obtain different failure modes, were prepared for the tests. Based on the experimental work, transition of natural mode shapes due to development of the cracks, as well as relationships between fundamental frequency and experienced maximum drift angle were successfully clarified. A series of results presented herein indicated the following findings.

- Flexural cracks that accompanied with the yielding of the longitudinal reinforcements were able to be detected based on the reduction of natural frequency. However further flexural damage such as the exfoliation of concrete and the local buckling of reinforcements was unlikely identified because further change of the frequency was quite limited.
- Although the natural mode shape changed to more complex one to recognize some local vibration modes excited around the potion damaged with the shear cracks, it seemed that the fundamental natural frequency was less affected by the occurrence of shear failure.
- Because evaluation of the cracks with yielding of reinforcements was more difficult than that of extensive damage such as flexural faire and shear failure in visual inspection, the vibration-based method is considered to be effective especially for evaluation of very important structures that require high integrity.

REFERENCES

Aktan, A. E., Catbas, F. N., Grimmelsman, K. A. and Tsikos, C. J. (2000). Issues in infrastructure health monitoring for management. *Journal of Engineering Mechanics*, ASCE, **126 (7)**, pp.711-724.

Housner, G., Bergman, L.A., Caughey, T.K., Chassiakos, A.G., Claus, R.O., Masri, S.F., Skelton, R.E., Soong, T.T., Spencer, B.F. and Yao, J.T.P. (1997). Special issue: Structural control: past, present, and future. *Journal of Engineering Mechanics*, ASCE, **123(9)**, 897-971.

Kanazawa, K. and Hirata, K. (2005). Parametric estimation of the cross power spectral density. *Journal of Sound and Vibration*,**Vol. 282**, **No. 1**, 235, 1-35.

Kanazawa, K. Kirita, F., Kitamura, H. and Matuoka, Y. (2008). Health monitoring of 4-story steel moment frame before and after the collapse test. *14th World Conference on Earthquake Engineering*, **S17-01-006**.

Miyagawa, Y. and Matumura. (2011). Damage evaluation of reinforced concrete underground structures after earthquake, CRIEPI-Report, **N11005** (in Japanese).

Nagata, S., Kanazawa, K., Yabana, S., Ukion, H. and Kajiwara, K. (2009). A long-term ambient vbiration monitoring on a shaking table test of a full-scale bridge. CRIEPI-Report, **N08033** (in Japanese).

Neild, S.A., Williams, M.S. and McFadden, P.D. (2002). Nonlinear behavior of reinforced concrete beams under low-amplitude cyclic and vibration loading. *Engineering Structures*, **24**, pp.707-718.

Neild, S.A., Williams, M.S. and McFadden, P.D. (2003). Nonlinear vibration charactaristics of damaged concrete beams. *Journal of Structural Engineering*, ASCE, **129 (2)**, pp.260-268.

Niwa, J., Yamada, K., Yokozawa, K. and Okamura, H.(1986). Reevaluation of the equation for shear strength of reinforced concrete beams without web reinforcement. *Journal of Structural Engineering/Earthquake Engineering*, JSCE, **372/V-5**, 167-176 (in Japanese).

Rens, K. L., Wipf, T. J. and Klaiber, F. W. (1997). Review of nondestructive evaluation technique of civil infrastructure. *Journal of Performance Constructed Facilities*, ASCE, **11(4)**, 152-160.

Rytter, A.(1993). Vibration based inspection of civil engineering structures. Doctoral dissertation, Department of building technology and structural engineering, University Aalborg, Aalborg, Denmark.

Seki, M., Mizutani, K., Nishimura, T. and Nakano, S.(1996). Characteristic vibration of rigid frame brides damaged by the Hyogo-ken-nanbu Earthquake. *Journal of Structural Engineering/Earthquake Engineering*, *JSCE*, **550/V-33**, 145-154 (in Japanese).

Seki, M., Nishimura, A., Sano, H. and Nakano, S.(2003). Study on the evaluation of damage levels of RC rigid frame railway bridges in the case of earthquakes. *Journal of Structural Engineering/Earthquake Engineering*, *JSCE*, **731/I-63**, 51-64 (in Japanese).

Uehan, F. and Meguro, K. (2004). Assessment of seismic damage to railway structures using applied element method and microtremor measurement. *13th World Conference on Earthquake Engineering*, **1407**.